Contribution from the Department of Chemistry, William Marsh Rice University, Houston, Texas 77001, and the School of Chemical Sciences, University of Illinois, Urbana, Illinois 61801

Electronic Spectral Study of Some Iron(II) Magnetic Isomers in Solution and a Spectral-Structural Correlation with Their Nickel(II) Analogs

LON J. WILSON,*[1] DANAE GEORGES,[2] and MITCHELL A. HOSELTON[3]

Received March 20, 1975 AIC50208N

Pseudooctahedral Fe(II) complexes of the hexadentate ligand tris[4-[(6-R)-2-pyridyl]-3-aza-3-butenyl]amine, where R is either H or CH_3, have been studied in solution by electronic spectroscopy. The complexes represent a magnetically interesting series with Fe–I being low-spin, Fe–IV high-spin, and Fe–II and Fe–III spin equilibrium species. The d–d electronic spectrum of high-spin Fe–IV has been interpreted in terms of a strongly distorted octahedral ligand field model with $10Dq = 11{,}400$ cm^{-1}. As evidenced by X-ray structural results, a major contribution of the reduction from O_h symmetry appears to arise from a *static* molecular distortion in which the average Fe–N(imine) and Fe–N(pyridine) bond distances differ by 0.14 Å. As for other low-spin tris(α-diimine)iron(II) complexes, the spectrum of Fe–I is characterized by only Fe(II) → ligand charge-transfer bands whose intensities and positions obscure any d–d transitions. The spectrum of the spin equilibrium Fe–III compound displays features commensurate with a mole-fraction-weighted population of both high-spin and low-spin magnetic isomers with $10Dq_{hs}$(Fe–III) being ~11,700 cm^{-1} when the two spin states are nearly equienergetic. The analogous Ni(II) complexes have also been synthesized and characterized by elemental analysis, infrared spectroscopy, and solution conductivity, magnetic susceptibility, ^1H NMR, and d–d electronic spectral measurements. From the spectral studies, $10Dq$ values for the series are found to increase according to the sequence Ni–IV (10,550 cm^{-1}) < Ni–III (11,000 cm^{-1}) < Ni–II (11,080 cm^{-1}) < Ni–I (11,240 cm^{-1}). Using spectral and available X-ray structural data for the two metal ion series, it has been empirically determined that $10Dq \propto r^{-1}$ with r the average M–N bond distance. From this structure–bonding relationship, a value of $10Dq_{ls}$ for Fe–I has been indirectly obtained, and ratios for $10Dq_{hs}(Fe^{2+})/10Dq(Ni^{2+})$ and $10Dq_{ls}(Fe^{2+})/10Dq(Ni^{2+})$ have been estimated as 1.07 and 1.15, respectively. By this ratio method, values of Dq_{hs} for Fe–II and Dq_{ls} for Fe–II and Fe–III have been obtained and a 3d-electron mean pairing energy, $\bar{P}$, calculated to be 12,800 ± 400 cm^{-1} for the family of Fe(II) complexes.

Introduction

Octahedral complexes of $3d^4$–$3d^7$ transition metal ions may exist in either high-spin or low-spin electronic configurations, depending upon the relative magnitudes of the ligand field splitting parameter, $10Dq$, and the 3d-electron mean pairing energy, $\bar{P}$. For metal ions possessing a $3d^6$ configuration, such as Fe(II), high-spin complexes occur when $10Dq << \bar{P}$ and low-spin complexes when $10Dq >> \bar{P}$. In a few rare situations, $10Dq \simeq \bar{P}$, and both the high-spin ($^5T_{2g}$ state of $t_{2g}^4e_g^2$ configuration) and the low-spin ($^1A_{1g}$ state of t_{2g}^6 configuration) electronic states may be thermally populated. Because the $^1A_{1g}$ state is diamagnetic and the $^5T_{2g}$ state is paramagnetic, the spin equilibrium process, $^1A_{1g} \rightleftarrows {}^5T_{2g}$, can be conveniently monitored by variable-temperature magnetic susceptibility studies. For this reason, spin equilibrium compounds are often said to exhibit magnetic isomerism. Detailed analysis of these variable-temperature magnetic data can be useful in characterizing the electronic structures of spin equilibrium processes in terms of such bonding parameters as $\Delta E(^1A_{1g} \rightarrow {}^5T_{2g})$, spin–orbit coupling constants, Zeeman effects, and the degree of molecular distortion from cubic symmetry.[4,5] Because such studies yield much information about electronic structure of metal complexes that is otherwise unavailable, spin equilibrium systems are of considerable interest and have been thoroughly studied whenever encountered. In addition, the presence of magnetic isomerism *in solution* offers an intriguing opportunity to obtain information about such electronic parameters as electron-pairing energies, *intra*molecular spin interconversion rates and the role of spin multiplicity changes on *inter*molecular electron-transfer processes. For such investigations, the study of magnetic isomerism will first have to be systematically extended into the solution state, since, to date, studies have been limited almost exclusively to the solid state.[4,5]

In the literature only eight uniquely different spin equilibrium systems of pseudooctahedral Fe(II) have been characterized: [Fe(1,10-phen)$_2$(NCS)$_2$],[6] [Fe(1,10-phen)$_2$(NCSe)$_2$],[6a] [Fe(2-Me-1,10-phen)$_3$]$^{2+}$,[7] the tris(2-aminomethylpyridine)iron(II) halides,[8] [Fe(2,2'-bpy)$_2$(NCS)$_2$],[6b,9] the 2-(2'-pyridyl)imidazoleiron(II) complexes,[10] the 2-(2-pyridylamino)-4-(2-pyridyl)thiazoleiron(II) series,[11] and the poly(1-pyrazolyl)borate–iron(II) system.[12] More recently, a new system has been reported by Hoselton, Wilson, and Drago[13] in which the Fe(II) complexes are derived from a single hexadentate ligand of the strong-field tris(α-diimine) variety. The synthesis and general structure of these complexes are outlined in Figure 1. The structures of compounds Fe–I, Fe–IV, and Ni–I, as shown in the figure, have been substantiated by single-crystal X-ray studies (Table II).[13b,32] These studies indicate that the Fe(II) complexes are best considered to be six-coordinate with the Fe–N_7 distances being too long (>3.30 Å) to be considered bonding in the usual sense. The magnetic and Mössbauer spectral properties have also been reported in detail,[13b] showing that compounds Fe–II, Fe–III, and Fe–IV, as their PF_6^- salts, are spin equilibrium compounds in the solid state while Fe–I is only low spin at all temperatures studied (4.2–300 K). More significant, however, is the fact that Fe–II and Fe–III were found to be the first Fe(II) complexes to display the spin equilibrium phenomenon as *ionic* species in solution.

The present study is largely concerned with the synthesis, characterization, and study of the analogous pseudooctahedral Ni(II) complexes of Figure I, Ni–I, Ni–II, Ni–III, and Ni–IV, as their PF_6^- salts. The electronic configuration of Ni(II) is $3d^8$, and while no spin equilibrium possibility exists for octahedral Ni(II), the d–d electronic spectra of such complexes are relatively well understood in terms of such ligand field bonding parameters as $10Dq$ and B, the Racah interelectronic repulsion parameter.[17] A solution-state electronic spectral study of the Ni(II) compounds of Figure 1 has, therefore, been undertaken with the intention of obtaining ligand field parameters for the [(6-Mepy)$_n$(py)$_m$tren] ligand set on Ni(II) which promote the high-spin, low-spin, and electronically novel spin equilibrium situation with Fe(II). In addition, the d–d electronic spectra of the high-spin Fe–IV and spin equilibrium Fe–III complexes have been obtained in solution and interpreted in terms of a strongly distorted octahedral ligand field model. Where possible, the spectral data for the Ni(II) and Fe(II) complexes have been correlated to structural information available from the single-crystal X-ray studies.

Experimental Section

Syntheses. Preparations for the [Ni(6-Mepy)$_n$(py)$_m$tren](PF$_6$)$_2$

Table I. Analytical Data for the $[M(6\text{-Mepy})_n(py)_m tren](PF_6)_2$ Complexes

Complex	% calcd C	% calcd H	% calcd N	% found C	% found H	% found N	Color
$[Ni(py)_3 tren](PF_6)_2$, Ni-I	37.82	3.57	12.86	38.06	3.81	12.81	Yellow-brown
$[Ni(6\text{-Mepy})(py)_2 tren](PF_6)_2$, Ni-II	38.68	3.76	12.63	38.75	3.79	12.63	Yellow-brown
$[Ni(6\text{-Mepy})_2(py) tren](PF_6)_2$, Ni-III	39.52	3.95	12.41	39.56	3.92	12.35	Yellow-green
$[Ni(6\text{-Mepy})_3 tren](PF_6)_2$, Ni-IV	40.29	4.14	12.19	40.32	3.75	11.82	Green
$[Fe(py)_3 tren](PF_6)_2$, Fe-I	37.96	3.58	12.91	38.17	3.52	12.86	Purple
$[Fe(6\text{-Mepy})(py)_2 tren](PF_2)_2$, Fe-II	38.82	3.78	12.68	38.75	3.75	12.75	Purple
$[Fe(6\text{-Mepy})_2(py) tren](PF_6)_2$, Fe-III	39.66	3.97	12.45	39.68	3.96	12.37	Reddish purple
$[Fe(6\text{-Mepy})_3 tren](PF_6)_2$, Fe-IV	40.44	4.15	12.24	40.36	4.20	12.23	Cherry red

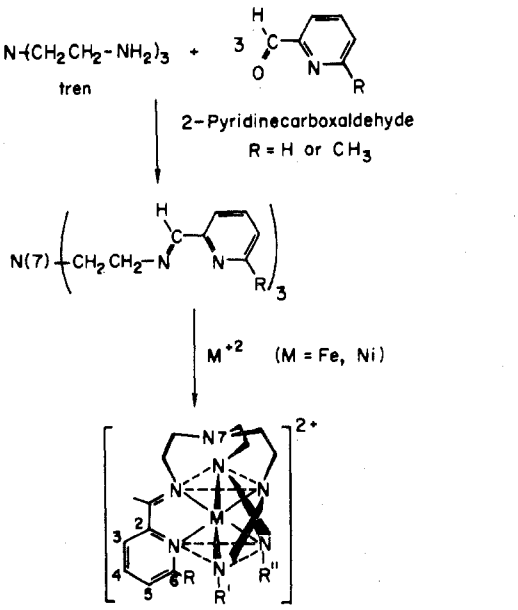

$[M(Py)_3 tren]^{2+}$; R = R' = R'' = H (M-I)

$[M(6\ Me\ Py)(Py)_2 tren]^{2+}$; R = R' = H, R'' = CH_3 (M-II)

$[M(6\ Me\ Py)_2(Py)\ tren]^{2+}$; R = H, R' = R'' = CH_3 (M-III)

$[M(6\ Me\ Py)_3\ tren]^{2+}$; R = R' = R'' = CH_3 (M-IV)

Figure 1. Synthesis and structure of the $[M(6\text{-Mepy})_n(py)_m tren](PF_6)_2$ complexes with M = Fe(II) or Ni(II).

compounds are similar to those reported for the analogous Fe(II) complexes.[13b] Analytical results for the compounds used in these studies are reported in Table I.

Physical Measurements. Infrared measurements on the solids were obtained with a Beckman IR-20 spectrophotometer as Nujol mulls in the range 4000–300 cm^{-1}.

Solution-state magnetic susceptibilities for the Ni(II) compounds were obtained by the NMR technique of Evans[14] in CH_3CN (shown in Table IV). Chloroform was used as the reference compound. μ_{eff} (BM) values were calculated using the equation μ_{eff} (BM) = $2.83[(\chi_M^{cor})T]^{1/2}$, where χ_M^{cor} is the corrected molar susceptibility (cgsu) and T the absolute temperature (K). The molar diamagnetic ligand corrections used in determining the values were calculated using Pascal's constants: $[(6\text{-Mepy})_n(py)_m tren]$ ligands, $\sim 190 \times 10^{-6}$ cm^3 mol^{-1}; PF_6^-, -64×10^{-6} cm^3 mol^{-1}. The solvent mass susceptibility values, χ_0, used in determining the χ_M^{cor} values were calculated using the equation $\chi_0 = K/d$, where K is the volumetric susceptibility and d is the density of the solvent in g/cm^3. The K value[15] used for CH_3CN was -0.534×10^{-6}. The temperature-dependent density equation[16] for CH_3CN was used in the calculation of χ_0.

Conductivity measurements for the PF_6^- salts were obtained at 25°C using a Beckman Model RC-18A conductivity bridge or a YSI Model 31 conductivity bridge.

Proton magnetic resonance spectra were obtained with a Varian Model HA/HR-60 spectrometer or Jeolco C60-H spectrometer operating in the HR mode, using a side-band calibration technique.

A Cary Model 17 recording spectrophotometer was used for measurements in the visible and near-infrared regions. The experimental electronic spectra were converted to a linear energy scale (cm^{-1}) and deconvoluted using a Du Pont Model 310 curve resolver programmed for gaussian distribution curves.

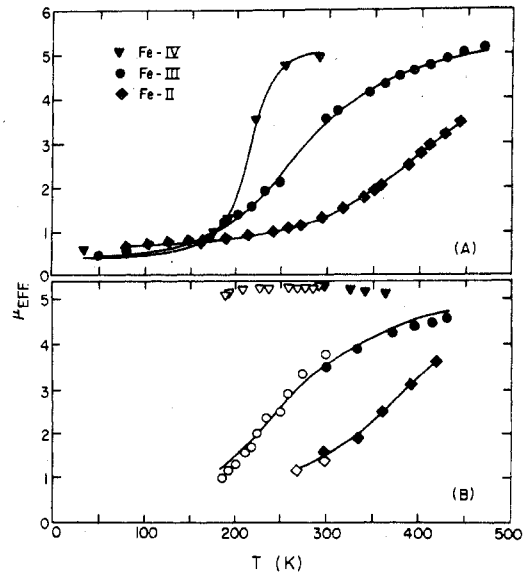

Figure 2. μ_{eff} (BM) vs. temperature (K) curves in the solid (A) and solution (B) states for the $[Fe(6\text{-Mepy})_n(py)_m tren](PF_6)_2$ complexes. In (B), open circles and squares are for acetone and solids for DMSO.

Chemical analyses were performed by the Microanalytical Laboratory of the School of Chemical Sciences, University of Illinois, and Galbraith Analytical Laboratories, Knoxville, Tenn.

Results and Discussion

The $[Fe(6\text{-Mepy})_n(py)_m tren](PF_6)_2$ series is electronically unique in that the members span a range from low-spin Fe(II) [$^1A_{1g}$ ground state; μ_{eff} (BM) ≈ 0)] to high-spin Fe(II) [$^5T_{2g}$ ground state; μ_{eff} (BM) = 4.9–5.2], depending on the R substitution pattern where R = H or CH_3. μ_{eff} (BM) vs. temperature (K) data for the series in both the solid and the solution states are shown in Figure 2. In the solid state, Fe–II, Fe–III, and Fe–IV exhibit a $^1A_1 \rightleftarrows {}^5T_2$ spin equilibrium process, while Fe–I is only low spin. The Fe–IV compound is the most thermochromic member of the series, changing in color from cherry red at room temperature to dark purple by 77 K. In solution, however, only Fe–II and Fe–III retain the spin equilibrium property with Fe–IV being exclusively high spin and Fe–I low spin over an approximately 200° temperature range. The presence of magnetic isomerism in the solution state for Fe–II and Fe–III is especially noteworthy since the only other Fe(II) complex known to exhibit spin equilibrium in both solid and solution states is compound ii of the iron(II) polyborate series[12] shown in Figure 3.

With the four members of the $[Fe(6\text{-Mepy})_n(py)_m tren](PF_6)_2$ series exhibiting such varied and unique magnetic behavior, it is desirable to obtain the ligand field parameters and other electronic factors, such as $10Dq$, B, and $\bar{P}$, that accompany the change in electronic structure. Unfortunately, such ligand field parameters for low-spin octahedral Fe(II) complexes cannot readily be obtained from electronic spec-

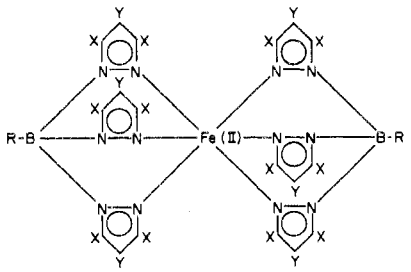

(i) R = 1-pyrazolyl; X=Y=H

(ii) R=H, X=Y=H

(iii) R=H, X=Y=CH_3

Figure 3. Structure of the polyborate-iron(II) complexes.

troscopy because intense Fe(II) → ligand charge-transfer bands in the visible and near-uv regions of the spectrum tend to obscure the relatively weak d–d bands. For this reason, the analogous $[Ni(6\text{-}Mepy)_n(py)_m tren]^{2+}$ series has been synthesized and studied with a view toward better understanding the changing structural and ligand field parameters that promote low-spin, high-spin, and spin equilibrium conditions within the analogous Fe(II) series. Through a comparison of structural and spectral data for the two metal ion series, it has been possible to establish the critical $10Dq_{hs}(Fe^{2+})/10Dq(Ni^{2+})$ and $10Dq_{ls}(Fe^{2+})/10Dq(Ni^{2+})$ ratios producing magnetic isomerism in the Fe(II) complexes and to obtain estimates of Dq_{ls} and Dq_{hs} for all of the pertinent low-spin and high-spin isomeric forms. Finally, it has also been possible to obtain an estimated value for P in these pseudooctahedral Fe(II) complexes.

Synthesis, Structure, and Characterization of the $[M(6\text{-}Mepy)_n(py)_m tren]^{2+}$ Series. The general procedure for the synthesis of the $[M(6\text{-}Mepy)_n(py)_m tren]^{2+}$ compounds (M = Ni(II) or Fe(II)) is essentially that as already reported for the Fe(II) species and is shown schematically in Figure 1. Synthesis of M–I and M–IV is straightforward, while the unsymmetrical M–II and M–III compounds are produced in a stepwise reaction scheme which is slightly more complicated. For example, the stepwise in situ syntheses of the unsymmetrical [(6-Mepy)$_2$(py)tren] and [(6-Mepy)(py)$_2$tren] ligands are based on the fact that primary amine groups undergo Schiff base condensation reactions with aldehydes, whereas amine hydrochloride salts are unreactive. By carefully controlling the amount of base added and the reaction conditions, the tren·3HCl salt can be deprotonated stepwise,[13b] permitting a highly selective condensation scheme with final compound yields of ~50%.

In addition to establishing the hexadentate nature of the ligands, the X-ray data in Table II also indicate that the effective molecular geometry of Fe–I is best described as a slightly distorted trigonal antiprism or octahedron. For the idealized geometry, the Fe(II) atom would lie in the center of the coordination polyhedron defined by the upper (three imine N's) and lower (three pyridine N's) triangular faces which would be twisted relative to one another by an angle $\theta = 60°$. The actual structure of Fe–I approaches the idealized polyhedron with $\theta(av) = 54°$ and the Fe–N(imine) and Fe–N(pyridine) distances of 1.94 and 1.97 Å being nearly equal. In fact, an octahedral assignment is probably as good an approximation for Fe–I as it is for the tris(1,10-phenanthroline)iron(II) complex where θ is also 54°.[32] For Fe–IV, with $\theta(av) = 51°$ and Fe–N(imine) and Fe–N(pyridine) bond distances of 2.14 and 2.28 Å at room temperature, the coordination polyhedron is somewhat more distorted but still reasonably well approximated by an octahedral model. Based on these X-ray results, variable-temperature magnetic susceptibility data for the solid-state spin equilibrium compounds Fe–II, Fe–III, and Fe–IV have been successfully interpreted using a trigonally distorted octahedral model with a trigonal distortion parameter δ_T of $\gtrsim$1000 cm^{-1} (as shown in Figure 7).[13b]

Table II. Selected Structural Parameters for Ni–I, Fe–I, and Fe–IV as PF_6^- Salts at Room Temperature

Compd	μ_{eff} at 300 K, BM	M–N-(pyridine),[c] Å	M–N-(imine),[c] Å	M–N-(7), Å	Av θ,[d] deg
Ni–I[a]	3.05	2.10	2.08	3.24	51
Fe–I[a]	0.50	1.97	1.94	3.44	54
Fe–IV[b]	5.00	2.28	2.14	3.31	51

[a] C. Mealli and E. C. Lingafelter, *Chem. Commun.*, 885 (1970); private communication from E. C. Lingafelter, University of Washington, Seattle, Wash. [b] Reference 13b. [c] Average of the three M–N distances. [d] θ is the twist angle between the two triangular faces described by the three imine nitrogen donor atoms and the three pyridine nitrogen donor atoms. $\theta = 60°$ in O_h symmetry.

It is of interest to note that the X-ray measurements also provide information about the mechanism involved in "fine tuning" the ligand field parameters into the region where the spin equilibrium may be observed. Calculations assuming Fe–N(pyridine) bond distances of 1.97 Å, as found in the X-ray structure of Fe–I, reveal that the carbon atom of a pyridine ring 6-methyl substituent would be expected to lie above the plane of a second pyridine ring at a N(pyridine)–C(methyl) contact distance of ~2.4 Å.[18a] This contact distance is well under the sum of the van der Waals radii for a nitrogen atom (1.5 Å) and a methyl group (2.0 Å). Therefore, it is presumed that this steric interaction accounts for the increased Fe–N bond distances in Fe–IV relative to those of Fe–I which, in turn, reduces $10Dq$ sufficiently to give rise to a high-spin ground state at 300 K. For Fe–II and Fe–III, the intermediate degrees of methyl substitution likely produce "averaged" Fe–N bond lengths and ligand field splittings intermediate between the Fe–I and Fe–IV extremes that give rise to the spin equilibrium magnetic property in both the solid and the solution states.

The results of the single-crystal X-ray study of Ni–I in Table II confirm that, with an average Ni–N(pyridine) distance of 2.11 Å, average Ni–N(imine) distance of 2.08 Å, and $\theta(av)$ = 51°, the Ni–I cation possesses the same general "capped" octahedral structure as do the Fe(II) complexes. The relatively long Ni–N$_7$ distance of 3.24 Å precludes any significant Ni–N$_7$ interaction, and Ni–I is, therefore, also considered to be a six-coordinate pseudooctahedral species. Wilson and Rose[18b] have verified the six-coordinate nature of Ni–I by showing the similarity of magnetic and electronic spectral properties of Ni–I with those of some closely related tris(α-diimine)nickel(II) chelates. Although X-ray data for Ni–II, Ni–III, and Ni–IV are presently lacking, these complexes are considered to possess the same general structural features as does the parent Ni–I compound. Furthermore, it is likely that Ni–IV also exhibits a trigonal distortion with M–N bond lengths comparable to those of its Fe(II) analog. This assumption seems reasonable in that *both* M–IV compounds are high spin with similar M(II) ionic radii and that the same *intra*ligand N(pyridine)–C(methyl) nonbonding interactions probably dominate the overall molecular geometry.

The new $[Ni(6\text{-}Mepy)_n(py)_m tren](PF_6)_2$ series has been completely characterized by elemental analysis, by infrared and uv–visible spectroscopy, and by solution conductivity, magnetic susceptibility, and contact shift ^1H NMR measurements. Analytical data, showing good agreement between calculated and found values for the $[Ni(6\text{-}Mepy)_n(py)_m tren](PF_6)_2$ complexes, are shown in Table I. The infrared spectral data in Table III for the Ni(II) series are

Table III. Infrared Spectral Data for the $[Ni(6\text{-}Mepy)_n(py)_m tren](PF_6)_2$ Complexes[a]

Assignment	Ni-I[b]	Ni-II	Ni-III	Ni-IV
C=N str	1652 s	1649 s	1659 s	1659 s
py band 1	1604 s	1602 s	1602 s	1603 s
py band 2	1574 w	1571 w	1571 w	1570 w
py band 3	1480 m	1476 m	1475 m	1480 m
py band 4	1440 s	1440 s	1438 s	1440 s

[a] Key: s, strong; m, medium; w, weak. All values in cm^{-1}; spectra run as Nujol mulls. [b] After L. J. Wilson and N. J. Rose, *J. Am. Chem. Soc.*, 90, 6041 (1968).

Table IV. Solution Magnetic Data for the $[Ni(6\text{-}Mepy)_n(py)_m tren](PF_6)_2$ Complexes in CH_3CN[a,b]

Compd	Temp, K	$10^{-3}\cdot\chi_M^{cor}$, cgsu	μ_{eff},[c] BM
$[Ni(py)_3tren](PF_6)_2$, Ni-I	321	3.26	2.90
$[Ni(6\text{-}Mepy)(py)_2tren]\cdot(PF_6)_2$, Ni-II	323	3.05	2.88
$[Ni(6\text{-}Mepy)_2(py)tren]\cdot(PF_6)_2$, Ni-III	323	3.54	3.04
$[Ni(6\text{-}Mepy)_3tren](PF_6)_2$, Ni-IV	323	3.53	3.04

[a] Measured by the Evans method in CH_3CN using chloroform as the reference compound (see Experimental Section). [b] Approximately 10^{-2} *M* in nickel compound. [c] Estimated error approximately 0.10 BM.

also consistent with the proposed structure of these complexes. The spectrum of Ni-I has been assigned[18b] on the basis of the pyridine and C=N stretching frequencies of the structurally related tris(α-diimine)nickel(II) complex tris(pyridinecarboxaldehyde methylimine)nickel(II) tetrafluoroborate as reported by Robinson, Curry, and Busch.[19] The pyridine and C=N stretching bands of Ni-II, Ni-III, and Ni-IV are found to occur at similar frequencies and with similar intensities as the corresponding bands in the Ni-I spectrum.

The magnetic moments of the $[Ni(6\text{-}Mepy)_n(py)_m tren]^{2+}$ series in CH_3CN are presented in Table IV. The values have been determined by the NMR technique of Evans (see Experimental Section) and are all within the 2.8–3.2 BM range characteristic of pseudooctahedral Ni(II) species with $^3A_{2g}$ ground states. In addition, conductivity measurements for the Ni(II) complexes in acetonitrile fall within the 363–377 ohm^{-1} $equiv^{-1}$ cm^2 range characteristic for 2:1 electrolytes in that solvent.[20]

The proton contact shift spectra for the $[Ni(6\text{-}Mepy)_n(py)_m tren]^{2+}$ series offer the most convincing proof for the existence of discrete monomeric species in solution. The spectra of Ni-I, Ni-II, Ni-III, and Ni-IV in CD_3CN are shown in Figure 4. Peak assignments are listed in Table V. For comparison, ^1H NMR data for the tris(2,2'-bipyridine)nickel(II), $[Ni(bpy)_3]^{2+}$, and the tris(pyridinecarboxaldehyde methylimine)nickel(II), $[Ni(PMI)_3]^{2+}$, cations have also been included in the table. The pyridine proton assignments have been made in accordance with those reported by Wicholas and Drago[21] for the $[Ni(bpy)_3]^{2+}$ complex and by Larsen et al.[22] for Ni-I. The spectrum of $[Ni(PMI)_3]^{2+}$ has been reported by Wilson and Bertini[23] and shows no multiplicity beyond that found for $[Ni(bpy)_3]^{2+}$. Therefore, the methine and *N*-methyl proton signals of the $[Ni(PMI)_3]^{2+}$ complex are apparently too broad and/or too far shifted to be observed. Furthermore, the $[Ni(6\text{-}Mepy)_n(py)_m tren]^{2+}$ spectra all show additional features and multiplicities which may be attributed to the presence of (1) the tren methylene protons, (2) the pyridine ring 6-methyl groups, or (3) the unsymmetrical nature of the Ni-II and Ni-III ligands.

The broad, slightly upfield resonance apparent in each of the four spectra in Figure 4 is assigned to the Hc and HD

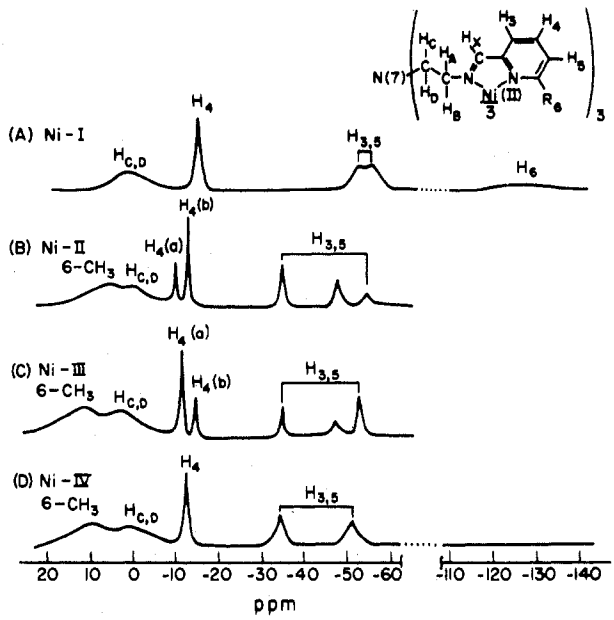

Figure 4. Proton magnetic resonance spectra of the $[Ni(6\text{-}Mepy)_n(py)_m tren](PF_6)_2$ complexes in CD_3CN at ~30°C. Reference is internal TMS with signal not shown.

Table V. Proton Magnetic Resonance Data for the $[Ni(6\text{-}Mepy)_n(py)_m tren]^{2+}$ and Related Tris(α-diimine)nickel(II) Complexes as PF_6^- Salts in CD_3CN at ~30°C

Compd	$\Delta\nu_4$	Shifts,[a,b] ppm $\Delta\nu_{3,5}$	$\Delta\nu_6$	$\Delta\nu_{C,D}$
Ni-I[c]	−15.1	−53.3	−128[f]	+1.6
		−56.8		
Ni-II[d]	−9.5 (a)	−32.4	[+4.1]	+2.2
	−11.7 (b)	−43.1		
		−49.4		
Ni-III[d]	−12.8 (a)	−53.0	[+11.2]	+2.0
	−14.8 (b)	−46.3		
		−35.3		
Ni-IV[c]	−13.1	−36.3	[+9.7]	+1.5
		−53.0		
$[Ni(bpy)_3]^{2+}$ [e]	−14.3	−44.7	−135[f]	
		−61.3		
$[Ni(PMI)_3]^{2+}$ [c]	−15.1	−48.5	−88.3[f]	
		−53.3		

[a] Shifts are relative to internal TMS: +, upfield; −, downfield. [b] See Figure 4 for the proton numbering scheme; methyl proton resonances are enclosed in brackets. [c] L. J. Wilson, Ph.D. Dissertation, University of Washington, Seattle, Wash., 1971. [d] This work. [e] After M. L. Wicholas and R. S. Drago, *J. Am. Chem. Soc.*, 90, 6946 (1968). [f] Resonances are very broad and accurate to only ±5 ppm.

methylenic protons of the tren bridgehead. The H_A and H_B protons are not expected to yield observable signals by analogy with the fact that a methyl proton signal is not observed for the $[Ni(PMI)_3]^{2+}$ complex. The upfield shift of Hc and HD for all the $[Ni(6\text{-}Mepy)_n(py)_m tren]^{2+}$ complexes can be rationalized in terms of a spin polarization mechanism similar to that described by Urbach for the related Ni(II) complex of *cis,cis*-1,3,5 tris(pyridine-2-carboxaldimino)cyclohexane.[24] The second broad upfield resonance in the spectra of Ni-II, Ni-III, and Ni-IV is assigned to the pyridine 6-methyl protons since its appearance is accompanied by the disappearance of the very broad 6-H resonance in the Ni-I spectrum. The 6-H signal, also expected to occur in the spectra of Ni-II and Ni-III, was too broad and of too low intensity to be resolved from the spectrum base line.

The upfield position of the methyl resonances for Ni-II, Ni-III, and Ni-IV is probably due to interaction of the methyl

Table VI. Electronic Spectral Data in CH_3CN and Calculated Ligand Field Parameters for the $[Ni(6\text{-}Mepy)_n(py)_m tren](PF_6)_2$ Complexes Assuming O_h Symmetry

Compd	ν_1, cm^{-1} (ϵ) $^3T_{2g}(F) \leftarrow {}^3A_{2g}$	ν', cm^{-1} (ϵ) $^1E_g(D) \leftarrow {}^3A_{2g}$	ν_2, cm^{-1} (ϵ) $^3T_{1g}(F) \leftarrow {}^3A_{2g}$	$10Dq$, cm^{-1}	P,[a] cm^{-1}	B,[b] cm^{-1}	β,[c] %
$[Ni(py)_3tren](PF_6)_2$, Ni-I	11,240 (3.1)	12,550 (2.6)	18,080 (7.1)	11,240	13,985	932	11
$[Ni(6\text{-}Mepy)(py)_2tren](PF_6)_2$, Ni-II	11,080 (3.5)	12,480 (2.9)	17,800 (6.0)	11,080	13,666	911	13
$[Ni(6\text{-}Mepy)_2(py)tren](PF_6)_2$, Ni-III	11,000 (4.6)	12,530 (1.1)	17,220 (5.2)	11,000	11,529	768	28
$[Ni(6\text{-}Mepy)_3tren](PF_6)_2$, Ni-IV	10,550 (3.4)	12,300 (0.8)	16,200 (4.8)	10,550	9,923	662	37

[a] Energy separation between the Ni(II) ^3P and ^3F states. [b] Racah parameter where $B = P/15$. [c] Percent lowering of P relatively to the Ni(II) free-ion value of 15,840 cm^{-1}.

protons with the π network of the adjacent pyridine ring; Wicholas[25] has proposed such a mechanism to account for the upfield shift of +15.8 ppm observed for the methyl resonance of $[Ni(2,9\text{-}dmp)_2(NO_3)_2]$ (2,9-dmp = 2,9-dimethylphenanthroline), in which the methyl substituent of one pyridine ring lies near enough to a second pyridine ring to cause a significant shielding interaction of the methyl protons by the pyridine π network.

The narrowest signals in the spectra of Figure 4 are due to the pyridine H_4 protons. The singlet nature of the H_4 resonances in spectra A and D is consistent with three equivalent chelate arms, reflecting the C_3 trigonal symmetry of the Ni–I and Ni–IV complexes in solution. However, spectra B and C both show *two* H_4 proton resonances (labeled $H_4(a)$ and $H_4(b)$ in Table V and Figure 4) with one signal having approximately twice the integrated intensity of the other. This doublet feature for the Ni–II and Ni–III H_4 resonance is reconcilable in terms of a lowering of molecular symmetry, where one chelate arm is dissimilar from the other two. The H_3 and H_5 resonances for Ni–II and Ni–III also show additional multiplicity associated with the nontrigonal symmetry for the two compounds, although the pattern is more complex than for the H_4 signal.

Electronic Spectra of the $[Ni(6\text{-}Mepy)_n(py)_m tren]^{2+}$ Complexes. Figure 5 shows the d–d electronic absorption spectra in the 7000–20,000-cm^{-1} region for the $[Ni(6\text{-}Mepy)_n(py)_m tren](PF_6)_2$ salts in CH_3CN. The spectra in the figure closely resemble those already reported for Ni–I[18,22] and for a series of closely related tris(α-diimine)nickel(II) chelates such as the $[Ni(bpy)_3]^{2+}$ cation and the tris(pyridinecarboxaldehyde methylimine)nickel(II) complex, $[Ni(PMI)_3]^{2+}$.[19] Furthemore, Palmer and Piper, in their single-crystal polarized spectral study of $[Ni(bpy)_3]^{2+}$, have argued convincingly for using an O_h model for the spectrum assignment,[26] even though the actual molecular symmetry can be no higher than D_3. Because the spectra of the $[Ni(6\text{-}Mepy)_n(py)_m tren]^{2+}$ series closely resemble those of $[Ni(bpy)_3]^{2+}$ and other tris(α-diimine)nickel(II) species, their assignment has also been tentatively based on the O_h ligand field model. In none of the Ni(II) solution spectra are additional splittings of the O_h ligand field bands due to a trigonal component evident. This result is in direct contrast to the d–d spectrum of the high-spin Fe–IV species, as is discussed below.

For the Ni(II) d^8 electronic configuration in an O_h ligand field, three spin-allowed transitions are expected to occur from a $^3A_{2g}(F)$ ground state. The spin-allowed transition of lowest energy, ν_1, is $^3T_{2g}(F) \leftarrow {}^3A_{2g}(F)$ and is equal to $10Dq$. The second, ν_2, is $^3T_{1g}(F) \leftarrow {}^3A_{2g}(F)$. The highest energy transition, ν_3, is $^3T_{1g}(P) \leftarrow {}^3A_{2g}(F)$. In addition to the three spin-allowed transitions, a spin-forbidden transition from the triplet ground state to a singlet state, $^1E_g(D) \leftarrow {}^3A_{2g}(F)$, or ν', may occur if such a transition is close in energy to a spin-allowed transition. Table VI summarizes the electronic spectral data, assignments, and other calculated parameters[17] for the $[Ni(6\text{-}Mepy)_n(py)_m tren]^{2+}$ series based on an O_h ligand field model. As for other tris(α-diimine)nickel(II) chelates, ν_3 is apparently obscured by the intense charge-transfer band in the near-uv region, while ν_2 coincides with the tail of this

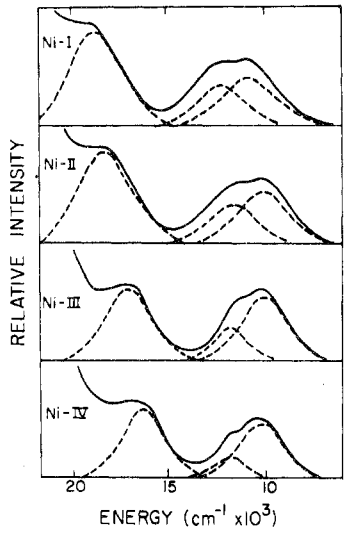

Figure 5. d–d electronic spectra of the $[Ni(6\text{-}Mepy)_n(py)_m tren](PF_6)_2$ complexes in CH_3CN at room temperature.

charge-transfer band. The latter fact makes the exact position of ν_2, as shown in Figure 5, somewhat uncertain. The low-energy absorption envelope from 7000 to 12,000 cm^{-1} appears to consist of two closely spaced transitions with one undoubtedly being ν_1 and the other probably ν'. Resolution of this broad absorption envelope can be arbitrary, and the relative position and assignment of the two bands have generated some controversy.[19,26] However, for the $[Ni(6\text{-}Mepy)_n(py)_m tren]^{2+}$ series, where the spectral changes appear stepwise and gradual, the ν' and ν_1 assignments have been made with considerable certainty since (1) the position of the ν' band should be of nearly constant energy in cases for strong-field ligands such as α-diimines, (2) the intensity of the spin-forbidden ν' transition should increase with its proximity to the spin-allowed ν_1 band, and, finally, (3) from the magnetic properties of the Fe(II) series, it is expected that Dq/B(M–I) > Dq/B(M–II) > Dq/B(M–III) > Dq/B(M–IV). Keeping these considerations in mind, the most reasonable deconvolution pattern and assignment for ν' and ν_1 is that shown in Figure 5 and given in Table VI.

In the Ni–I spectrum of Figure 5, ν' and ν_1 have nearly equal intensities and the reverse assignments from those appearing in Table VI were previously made.[18,22] A most interesting result of the present spectral study is the gradual 690-cm^{-1} reduction in $10Dq$ for the series in going from Ni–I to the Ni–IV complex. This decrease in $10Dq$ with increasing number of 6-methyl substituents undoubtedly results from the same methyl group–pyridine ring steric interactions that produce the gradual low-spin to high-spin conversion in the Fe(II) series. It is also interesting to note that the $10Dq$ values decrease in a monotonic though nonlinear fashion with the number of pyridine ring methyl groups. As expected, the three methyl groups in the M–IV complexes produce the largest steric demand within the series as evidenced by the large change of $\Delta(10Dq) = 450$ cm^{-1} in going from Ni–IV to Ni–III

Table VII. Solution Magnetic and Electronic Spectral Data for the Iron(II) Polyborate Complexes at Room Temperature[a]

Compd[b]	Solvent	μ_{eff}, BM	ν, cm^{-1}	ϵ	Assignment
i	$CHCl_3$	~0	18,900	90	$^1T_{1g} \leftarrow {}^1A_{1g}$ (low spin)
			29,200	13,700	Metal → ligand charge transfer
ii	CH_2Cl_2	2.71	18,700	57	$^1T_{1g} \leftarrow {}^1A_{1g}$ (low spin)
			29,700	12,100	Metal → ligand charge transfer
iii	C_6H_6	5.2	12,500	3.2	$^5E_g \leftarrow {}^5T_{2g}$ (high spin)
			44,000	39,000	Metal → ligand charge transfer

[a] Data taken from ref 12. [b] See Figure 3 for ligand structures.

as compared to the smaller change in going either from Ni–III to Ni–II (80 cm^{-1}) or from Ni–II to Ni–I (160 cm^{-1}).

If it is assumed, as argued above, that the Ni–N(imine) and Ni–N(pyridine) bond distances in Ni–IV are about the same as those in the corresponding high-spin Fe–IV complex (Table II), it is possible to develop an empirical relationship between $10Dq$ and the average Ni–N bond distances for the $[Ni(6\text{-}Mepy)_n(py)_m tren]^{2+}$ series. For example, assuming that $10Dq \propto r^{-n}$, where r is the average Ni–N bond distance, the portionality relationship

$$\frac{10Dq(\text{Ni-I})}{10Dq(\text{Ni-IV})} = \frac{r^{-n}(\text{Ni-I})}{r^{-n}(\text{Ni-IV})}$$

can be evaluated for the n power dependency of r. Using an average $r = 2.09$ Å value for Ni–I and the $10Dq$ values for Ni–I and Ni–IV as shown in Table VI, the relationship $10Dq \propto r^{-1}$ most closely satisfies the portionality expression for an assumed $r = 2.21$ Å value for Ni–IV. The actual calculated value of r for $n = 1$ is 2.23 Å, whereas other values of n such as 2, 3, 4, and 5, give increasingly less satisfactory calculated r values of 2.16, 2.14, 2.12, and 2.11 Å, respectively. A $10Dq \propto r^{-1}$ relationship is most interesting when compared to the r^{-5} or r^{-6} dependency which results from point charge or point dipole crystal field models[27] and is probably best viewed as empirically correct for these noncubic geometries with extensive metal–ligand covalent bonding. An X-ray structural study of Ni–IV is needed, however, to establish conclusively the underlying assumption of the above argument that $10Dq$ is indeed a linear function of r^{-1} for these Ni(II) complexes having Ni–N bond lengths of ~2.1–2.3 Å.

Unfortunately, the error involved in determining ν_2 in Figure 5 renders values calculated for P, and consequently for B and β,[17] rather uncertain. Because of this consideration, no detailed interpretation of P, B, and β has been attempted, although the calculated values are presented in Table VI. It should be noted, however, that Palmer and Piper[26] in their single-crystal study of $[Ni(bpy)_3]^{2+}$ calculated a value for B of 710 cm^{-1} or a 31% lowering of the repulsion parameter from the free-ion value. While this β (%) value is in especially good agreement with the values found for Ni–III and Ni–IV, the significance of this result is uncertain since the reverse ν_1 and ν' assignments were assumed for $[Ni(bpy)_3]^{2+}$.

Electronic Spectra of the $[Fe(6\text{-}Mepy)_n(py)_m tren]^{2+}$ Complexes. Other than the present $[Fe(6\text{-}Mepy)_n(py)_m tren]^{2+}$ species, the only other Fe(II) complex exhibiting magnetic isomerism in solution is the X = Y = R = H derivative of the substituted iron(II) polyborates (Figure 3) reported by Jesson, Trofimenko, and Eaton.[12] In solution at room temperature, compound i is low spin, iii is high spin, and ii is found to be of intermediate spin. No X-ray structural data are available for the polyborate series, but molecular models indicate that intramolecular ligand steric interactions are not an important factor in the complexes, and the variable magnetic properties, therefore, arise solely from ligand substituent electronic effects. Thus the mechanism giving rise to magnetic isomerism in these complexes is different from that of $[Fe(6\text{-}Mepy)_n(py)_m tren]^{2+}$ series where steric effects are largely responsible for the phenomenon.

Table VIII. Magnetic and Electronic Spectral Data for the Fe-I, Fe-III, and Fe-IV Complexes in CH_3CN[a]

Compd	μ_{eff}, BM	ν, cm^{-1}	ϵ	Assignment
Fe-I	0.5	17,920	7040	Metal → ligand charge transfer
		~19,230 sh		
Fe-III	3.7	17,300	7549	Metal → ligand charge transfer
		~19,230 sh		
		~11,700[b]	~13	$^5E_g \leftarrow {}^5T_{2g}$ (high-spin component)
Fe-IV	5.0	20,408	1165	Metal → ligand charge transfer
		11,400[c]	23.5	$^5E_g \leftarrow {}^5T_{2g}$ (high spin)

[a] Determined at 300 K. [b] Shoulder at base of intense charge-transfer band shown in Figure 6 (B). [c] Approximate center of unsymmetrical band shown in Figure 6 (A).

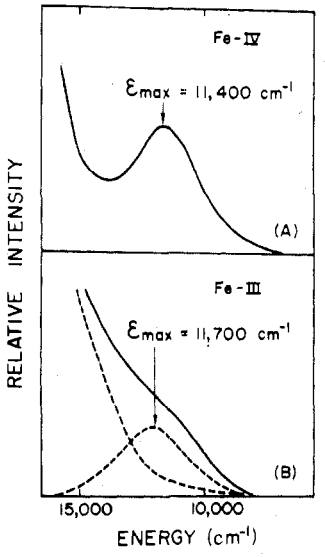

Figure 6. d–d electronic spectra of Fe-IV (A) and Fe-III (B) in CH_3CN at 300 K.

The electronic spectra of the polyborate complexes have been assigned employing the Tanabe–Sugano energy level diagram for a d^6 ion in an octahedral ligand field.[12] The spectral data and band assignments are reproduced in Table VII. Due to the relatively low intensity of the 18,900-cm^{-1} band in the spectrum of the low-spin complex i, this transition was assigned as $^1T_{1g} \leftarrow {}^1A_{1g}$. The much higher intensity and higher energy transition for the complex at 29,200 cm^{-1} was attributed to a Laporte-allowed metal → ligand charge transfer. In the spectrum of the high-spin complex iii, the low-intensity symmetrical band at 12,500 cm^{-1} was assigned to the $^5E_g \leftarrow {}^5T_{2g}$ transition. Although complex ii is of intermediate spin in solution, its spectrum was also assigned after the spectrum of the fully low-spin complex i.

The electronic absorption spectral data for Fe–I, Fe–III, and Fe–IV are presented in Table VIII, and the electronic spectra in the 5000–17,000-cm^{-1} range for Fe–III and Fe–IV in CH_3CN are shown in Figure 6. Unlike for the low-spin polyborate–iron(II) compound i, no d–d band attributable to

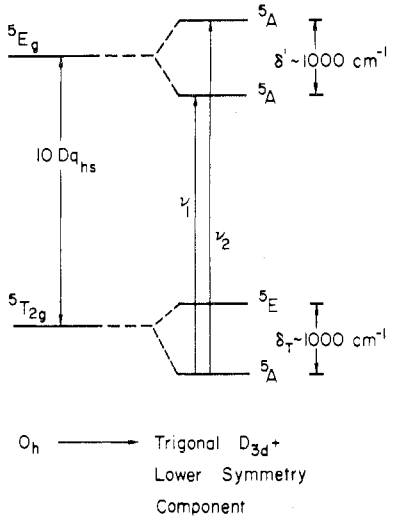

Figure 7. Energy level diagram for the high-spin d^6 electronic configuration in an O_h ligand field. Splitting of $^5T_{2g}$ under a trigonal distortion was estimated from ref 13b. Splitting of ^5E_g when symmetry is less than D_{3d} is estimated from d–d spectral data of this work.

a $^1T_{1g} \leftarrow {}^1A_{1g}$ transition is observed in the spectrum of Fe–I where, apparently, the intense metal → ligand charge-transfer band centered at 17,920 cm^{-1} ($\epsilon \sim 7000$) completely obscures the transition. As in the case for the high-spin polyborate complex iii, a low-intensity absorption attributable to the $^5E_g \leftarrow {}^5T_{2g}$ transition is found at 11,400 cm^{-1} in the spectrum of the fully high-spin Fe–IV. The spectrum is shown in Figure 6(A). For an octahedral high-spin Fe(II) complex of d^6 electronic configuration, the energy of the $^5E_g \leftarrow {}^5T_{2g}$ transition is equal to $10Dq$.[28] This band assignment and resulting value of $10Dq = 11{,}400$ cm^{-1} for the Fe–IV complex seems reasonable in view of the 10,550-cm^{-1} value as measured for the analogous Ni–IV complex. However, an interesting feature of the $^5E_g \leftarrow {}^5T_{2g}$ band is that it appears *unsymmetrical*, having a low-energy shoulder. Although no formal attempt has been made to resolve this band into two components, such a deconvolution would result in two bands separated by approximately 1000–1200 cm^{-1}. The origin of the unsymmetrical absorption envelop is uncertain but is tentatively attributed to either (1) an additional *static* molecular distortion which reduces the microsymmetry about the Fe(II) ion to something less than the D_{3d} trigonal distortion or (2) to a *dynamic* Jahn–Teller type distortion. In either case, the octahedral ^5E_g state could be split into two components differing in energy by as much as $\gtrsim 1000$ cm^{-1}.[28,29] Figure 7 shows the energy level diagram that results by assuming a D_{3d} trigonal distortion ($\delta_T \sim 1000$ cm^{-1}) superimposed upon the O_h field and the additional splitting ($\delta' \sim 1000$ cm^{-1}) of the ^5E_g octahedral state. Although it is not shown in the figure, the degeneracy of the $^5E(^5T_{2g})$ could also be lifted by the δ'-type distortion. The $\delta_T \sim 1000$ cm^{-1} splitting has been estimated from variable-temperature susceptibility measurements[13b] while the $\delta' \sim 1000$ cm^{-1} splitting seems reasonably to explain the unsymmetrical nature of the $^5E_g \leftarrow {}^5T_{2g}$ band as actually consisting of the two components, ν_1 and ν_2, shown in Figure 7.

It is interesting to compare the spectroscopic results for the Fe(II) and Ni(II) [(6-Mepy)$_n$(py)$_m$tren] series in a manner similar to that of Robinson, Curry, and Busch, who compared $10Dq$ values for the octahedral Ni(II) complexes of chloride, water, 2-pyridinecarboxaldehyde dimethylhydrazone, ammonia, and ethylenediamine with the $10Dq$ values of the corresponding high-spin octahedral Fe(II) complexes.[19] From this series of compounds these workers noted a $10Dq_{hs}(Fe^{2+})/10Dq(Ni^{2+})$ ratio of 1.11 ± 0.07. A ratio of 1.08 as calculated for Fe–IV and Ni–IV falls well within this range. The spectrum of Fe–III, which exhibits a $^1A_{1g} \rightleftarrows {}^5T_{2g}$ spin equilibrium in solution, is magnetically the most interesting member of the series. In this case, the electronic spectrum is expected to be a composite of the low-spin and high-spin spectra since the spin interconversion rates for the $^1A_{1g} \rightleftarrows {}^5T_{2g}$ process are known to be slow relative to the electronic transition time scale.[30] As seen from Table VIII, this is the case for Fe–III where bands attributable to both the $^5T_{2g}$ and $^1A_{1g}$ spin states are observed at 300 K. The $^5E_g \leftarrow {}^5T_{2g}$ transition of the high-spin form is of particular interest. As seen in Figure 6(B), it occurs just before the onset of an intense metal → ligand charge-transfer band and its position and intensity can, therefore, only be estimated at ~11,700 cm^{-1} ($\epsilon \sim 13$). This value is 300 cm^{-1} higher in energy than for the $^5E_g \leftarrow {}^5T_{2g}$ ($=10Dq_{hs}$) transition in Fe–IV and represents the increase in the ligand field strength producing conversion from a high-spin to a spin equilibrium "ground state" at 300 K. The $10Dq$ value for the corresponding Ni–III compound is 11,000 cm^{-1}, and the $10Dq_{hs}(Fe^{2+})/10Dq(Ni^{2+})$ ratio in this case is, therefore, 1.06. Here again the $10Dq$ ratio value falls well within the range determined by Robinson et al. but represents a considerable refinement of the critical $10Dq_{hs}(Fe^{2+})/10Dq(Ni^{2+})$ ratio corresponding to production of magnetic isomerism in, at least, these Fe(II) spin equilibrium complexes.

Experimental Estimation of a 3d-Electron Mean Pairing Energy for Fe(II). If a d–d electronic spectrum is observed, spin equilibrium compounds offer the unique possibility of experimentally estimating 3d-electron mean pairing energies, $\bar{P}$. In general, solution spectral measurements seem preferable to solid-state measurements due to enhanced band resolution and the possibility of calculating band intensities for assignment purposes. Solution-state spin equilibria of the type displayed by Fe–II and Fe–III are, therefore, primary candidates for such studies. Assuming O_h symmetry for Fe–III, the crystal field stabilization energy of the high-spin isomer is $-4Dq_{hs} + \bar{P}$ and for the corresponding low-spin isomer the energy is $-24Dq_{ls} + 3\bar{P}$. For conditions where the two spin states are nearly equienergetic, $E_{ls} \simeq E_{hs}$ or $\bar{P} \simeq [-4Dq_{hs} + 24Dq_{ls}]/2$. The calculation of $\bar{P}$, therefore, requires only values of Dq_{hs} and Dq_{ls} as determined from the d–d electronic spectra.

From the measured $10Dq_{hs}$ values for Fe–III and Fe–IV and the observed average $10Dq_{hs}(Fe^{2+})/10Dq(Ni^{2+})$ ratio of 1.07, the Dq_{hs} values for Fe–II, Fe–III, and Fe–IV are determined to be 1184, 1170, and 1140 cm^{-1}, respectively. Due to the unfavorable position of the Fe(II) → ligand charge-transfer bands, $10Dq_{ls}$ cannot be directly measured for any of these complexes. It is possible, however, to obtain an approximate value of $10Dq_{ls}$ for Fe–I from the r^{-1} dependence of $10Dq$ observed in the case of the $[Ni(6\text{-Mepy})_n(py)_m tren]^{2+}$ series. Solving the equation

$$\frac{10Dq_{ls}(\text{Fe-I})}{10Dq_{hs}(\text{Fe-IV})} = \frac{r^{-1}(\text{Fe-I})}{r^{-1}(\text{Fe-IV})} = \frac{1.95^{-1}}{2.21^{-1}}$$

$10Dq_{ls}$(Fe–I) is estimated as 12,900 cm^{-1}.[33] The new ratio $10Dq_{ls}(Fe^{2+})/10Dq(Ni^{2+})$ is thus determined to be 1.15. Estimates of Dq_{ls} for Fe–I, Fe–II, and Fe–III are then 1290, 1270, and 1260 cm^{-1}, respectively. With Dq_{ls} and Dq_{hs} values thus approximated, $\bar{P}$ is calculated to be 12,800 ± 400 cm^{-1}. A value of $\bar{P} = 12{,}800$ cm^{-1} for these Fe(II) complexes is somewhat greater than 12,000–12,500 cm^{-1} as estimated for other pseudooctahedral Fe(II) systems[12,31] but seem quite reasonable since $|10Dq_{ls} - \bar{P}| \simeq 200$ cm^{-1}, a necessary condition for observation of the spin equilibrium phenomenon over the temperature interval studied.

Acknowledgment. We thank the donors of the Petroleum Research Fund, Administered by the American Chemical

Society, and William Marsh Rice University (NASA Materials Grant NGR-44-006-001) for support of this work.

Registry No. Ni-I, 56348-41-5; Ni-II, 56348-43-7; Ni-III, 56348-45-9; Ni-IV, 56348-47-1; Fe-I, 55222-32-7; Fe-II, 55190-32-4; Fe-III, 55190-34-6; Fe-IV, 55190-36-8.

References and Notes

(1) William Marsh Rice University.
(2) William Marsh Rice University Fellow, 1973-1974.
(3) University of Illinois.
(4) R. L. Martin and A. H. White, *Transition Met. Chem.*, **4** (1968).
(5) E. K. Barefield, D. H. Busch, and S. M. Nelson, *Q. Rev., Chem. Soc.*, **22**, 457 (1968).
(6) (a) E. König and K. Madeja, *Inorg. Chem.*, **6**, 48 (1967); (b) A. J. Cunningham, J. E. Fergusson, H. K. J. Powell, E. Sinn, and H. Wong, *J. Chem. Soc., Dalton Trans.*, 2155 (1972).
(7) H. A. Goodwin and R. N. Sylva, *Aust. J. Chem.*, **21**, 83 (1968).
(8) G. A. Renovitch and W. A. Baker, Jr., *J. Am. Chem. Soc.*, **89**, 6377 (1967).
(9) E. König, K. Madeja, and K. J. Watson, *J. Am. Chem. Soc.*, **90**, 1146 (1968).
(10) D. M. L. Goodgame and A. A. S. C. Macado, *Inorg. Chem.*, **8**, 2031 (1969).
(11) R. N. Sylva and H. A. Goodwin, *Aust. J. Chem.*, **20**, 479 (1967).
(12) J. P. Jesson, S. Trofimenko, and D. R. Eaton, *J. Am. Chem. Soc.*, **89**, 3158 (1967).
(13) (a) M. A. Hoselton, R. S. Drago, N. Sutin, and L. J. Wilson, paper presented at the Southwest Regional Meeting of the American Chemical Society, Houston, Tex., Dec 1974; (b) M. A. Hoselton, L. J. Wilson, and R. S. Drago, *J. Am. Chem. Soc.*, **97**, 1722 (1975).
(14) D. F. Evans, *J. Chem. Soc.*, 2003 (1959).
(15) Ya. G. Dorfman, "Diamagnetism and the Chemical Bond", American Elsevier, New York, N.Y., 1965, pp 113 and 153.
(16) National Research Council, "International Critical Tables of Numerical Data, Physics, Chemistry, and Technology", Vol. III, 1st ed, McGraw-Hill, New York, N.Y., 1928, pp 27-30.
(17) R. S. Drago, "Physical Methods in Inorganic Chemistry", Van Nostrand-Reinhold, New York, N.Y., 1965, pp 410-411.
(18) (a) L. J. Wilson, Ph.D. dissertation, University of Washington, Seattle, Wash., 1971; (b) L. J. Wilson and N. J. Rose, *J. Am. Chem. Soc.*, **90**, 6041 (1968).
(19) M. A. Robinson, J. D. Curry, and D. H. Busch, *Inorg. Chem.*, **2**, 1178 (1963).
(20) L. V. Interrante, *Inorg. Chem.*, **7**, 943 (1968).
(21) M. L. Wicholas and R. S. Drago, *J. Am. Chem. Soc.*, **90**, 6946 (1968).
(22) E. Larsen, G. N. La Mar, B. E. Wagner, J. E. Parks, and R. H. Holm, *Inorg. Chem.*, **11**, 2652 (1972).
(23) L. J. Wilson and I. Bertini, *J. Coord. Chem.*, **1**, 237 (1972).
(24) S. O. Wandiga, J. E. Sarneski, and F. L. Urbach, *Inorg. Chem.*, **11**, 1349 (1972).
(25) M. L. Wicholas, *Inorg. Chem.*, **10**, 1086 (1971).
(26) R. A. Palmer and T. S. Piper, *Inorg. Chem.*, **5**, 864 (1966).
(27) See for example J. H. Van Vleck, *J. Chem. Phys.*, **7**, 72 (1939); B. N. Figgis, "Introduction to Ligand Fields", Interscience, New York, N.Y., 1966, p 38.
(28) F. A. Cotton and M. D. Meyers, *J. Am. Chem. Soc.*, **82**, 5023 (1960).
(29) *Ann. Phys. (N.Y.)*, **3**, 304 (1958).
(30) First-order rate constants for the

$$^1A_{1g} \underset{k_{-1}}{\overset{k_1}{\rightleftharpoons}} {}^5T_{2g}$$

process have recently been measured by a laser temperature-jump technique: M. A. Hoselton, N. Sutin, R. S. Drago, and L. J. Wilson, Abstracts, Southwest Regional Meeting of the American Chemical Society, Houston, Tex., Dec 1974; also to be submitted for publication. For Fe-III, k_1 and k_{-1} values in acetone (10%)-water at 21°C are $\sim 6 \times 10^5$ and $\sim 8 \times 10^6$ sec^{-1}, respectively. The spin interconversion process for Fe-III is, therefore, measurably *slower* than for ii of the polyborate-iron(II) complexes (Figure 3) where k_1 and k_{-1} are 1×10^7 and 2×10^7 sec^{-1}: J. K. Beattie, N. Sutin, D. H. Turner, and G. W. Flynn, *J. Am. Chem. Soc.* **95**, 2052 (1973).
(31) See, for example, E. König and S. Kremer, *Theor. Chim. Acta.*, **23**, 12 (1971).
(32) C. Mealli and E. C. Lingafelter, *Chem. Commun.*, 885 (1970); E. C. Lingafelter, private communication.
(33) Using an r^{-5} dependency, as proposed for [Fe(bpy)$_2$(NCS)$_2$] (E. König and K. J. Watson, *Chem. Phys. Lett.*, **6**, 456 (1970)), gives an unacceptably large value for $10Dq_{ls}$(Fe-I) of 21,300 cm^{-1}.

Contribution from the Department of Chemistry, The University of British Columbia, Vancouver, British Columbia, V6T 1W5, Canada

Cobalt-59 Nuclear Quadrupole Resonance of Derivatives of Dicobalt Octacarbonyl

LIAN SAI CHIA,[1] WILLIAM R. CULLEN,* MICHAEL C. L. GERRY,* and EDWARD C. LERNER[1]

Received June 5, 1975 AIC50401H

The ^{59}Co nuclear quadrupole resonance spectra of a number of derivatives of dicobalt octacarbonyl are reported. These include the complexes (RC≡CR')Co$_2$(CO)$_6$ (R = R' = H, CF$_3$, CH$_2$OH, C$_6$H$_5$; R = H, R' = C(CH$_3$)$_3$), the norbornadiene derivatives (π-C$_7$H$_8$)Co$_2$(CO)$_6$ and (π-C$_7$H$_8$)$_2$Co$_2$(CO)$_4$, and the ligand-bridged f$_4$farsCo$_2$(CO)$_6$ and f$_4$fars(C$_6$H$_5$C≡CC$_6$H$_5$)Co$_2$(CO)$_4$. The parameters obtained from the spectra of the alkyne complexes are related to the electronegativities of R and R' with e^2Qq being inversely proportional to η. The data indicate that the sign of e^2Qq is different from that in Co$_2$(CO)$_8$. The two chemically different cobalt atoms in (π-C$_7$H$_8$)Co$_2$(CO)$_6$ do not have very different NQR parameters. These are similar to those derived for the other complexes with nonplanar Co$_2$(CO)$_2$ bridging systems but are different from those of (π-C$_7$H$_8$)$_2$Co$_2$(CO)$_4$ which reinforces the belief that this last complex is planar.

In recent years there has been an increasing interest in the application of nuclear quadrupole resonance (NQR) spectroscopy to structural and bonding problems.[2-4] Although ^{59}Co NQR spectra of a number of compounds have been reported,[4] most of these have been obtained from simple derivatives containing only one cobalt atom per molecule or ion. A notable exception is the NQR spectrum of dicobalt octacarbonyl, A, which has been discussed in detail.[5,6] This carbonyl reacts with group 5 donors and organic π donors with displacement of carbon monoxide.[7] Many of the products are axially symmetric derivatives of the type LCo(CO)$_3$-Co(CO)$_3$L (e.g., L = (C$_6$H$_5$)$_3$P) whose NQR spectra have been described recently.[4,8,9] However other products are often formed and have more complex structures such as B and C, obtained by treating alkynes and norbornadiene with the parent carbonyl A.[10-15] The purpose of the present investigation was to determine the NQR spectra of a variety of derivatives of A to ascertain if the technique would reveal (1) gross differences in structure (e.g., the two inequivalent cobalt atoms in C) and (2) more subtle electronic effects due to, for example, varying the nature of R and R' in B.

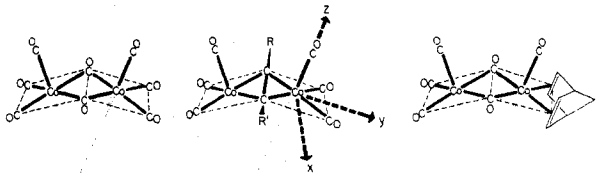

A B C

Experimental Section

All compounds were prepared by methods described in the literature.[12] The NQR spectra were recorded using a Decca instrument with Zeeman modulation. The minimum frequency obtainable was 7 MHz. The resonance frequencies were measured with the aid of